

## Evaluation of $^{18}\text{F}$ -labeled acetylcholinesterase substrates as PET radiotracers

Xia Shao,<sup>a</sup> Robert A. Koeppe,<sup>a</sup> Elizabeth R. Butch,<sup>b</sup>  
Michael R. Kilbourn<sup>a</sup> and Scott E. Snyder<sup>a,\*</sup>

<sup>a</sup>Division of Nuclear Medicine, Department of Radiology, University of Michigan Medical Center, Ann Arbor, MI 48109, USA

<sup>b</sup>Department of Chemistry, Eastern Michigan University, Ypsilanti, MI 48197, USA

Received 15 April 2004; revised 14 October 2004; accepted 14 October 2004

Available online 6 November 2004

**Abstract**—Four  $^{18}\text{F}$ -labeled acetylcholinesterase (AChE) substrates, (*S*)-*N*-[ $^{18}\text{F}$ ]fluoroethyl-2-piperidinemethyl acetate (**1**), (*R*)-*N*-[ $^{18}\text{F}$ ]fluoroethyl-3-pyrrolidinyl acetate (**2**), *N*-[ $^{18}\text{F}$ ]fluoroethyl-4-piperidinyl acetate (**3**), and (*R*)-*N*-[ $^{18}\text{F}$ ]fluoroethyl-3-piperidinyl acetate (**4**), were evaluated for in vivo blood and brain metabolism in mice, brain pharmacokinetics in rats monkeys (*M. nemistrina*) using PET imaging. All  $^{18}\text{F}$ -labeled compounds were compared to *N*-[ $^{11}\text{C}$ ]methyl-4-piperidinyl propionate (PMP). Compound **1** was completely metabolized within 1 min in mouse blood and brain. This compound had relatively fast regional brain pharmacokinetics and poor discrimination between brain regions with different AChE concentration. Compound **4** showed relatively slower blood metabolism and slower pharmacokinetics than compound **1** but again poor discrimination between brain regions. Both compounds **1** and **4** showed different kinetic profiles than PMP in PET studies. Compound **3** had the slowest blood metabolism and slower pharmacokinetics than PMP. Compound **2** showed highly encouraging characteristics with an in vivo metabolism rate, primate brain uptake, and regional brain pharmacokinetics similar to [ $^{11}\text{C}$ ]PMP. The apparent hydrolysis rate constant  $k_3$  in primate cortex was very close to that of [ $^{11}\text{C}$ ]PMP. This compound has potential to be a good PET radiotracer for measuring brain AChE activity. The longer lifetime of  $^{18}\text{F}$  would permit longer imaging times and allows preparation of radiotracer batches for multiple patients and delivery of the tracer to other facilities, making the technique more widely available to clinical investigators.  
© 2004 Elsevier Ltd. All rights reserved.

### 1. Introduction

Acetylcholinesterase (AChE) is the enzyme that catalyzes the degradation of the neurotransmitter acetylcholine, leading to the termination of cholinergic neurotransmission. Both clinical and postmortem studies indicated that the biochemical changes in brain of Alzheimer's disease (AD) include a progressive reduction in AChE activity.<sup>1–4</sup> Positron emission tomography (PET) is currently used to measure the AChE activity in vivo by imaging human brain with  $^{11}\text{C}$ -labeled radiotracers, *N*-[ $^{11}\text{C}$ ]methyl-4-piperidinyl acetate (AMP or MP4A), and *N*-[ $^{11}\text{C}$ ]methyl-4-piperidinyl propionate (PMP or MP4P).<sup>2–6</sup> Both esters serve as acetylcholinesterase substrates and are hydrolyzed to a hydrophilic product, *N*-[ $^{11}\text{C}$ ]methyl-4-piperidinol (MPOH), which

does not cross the blood–brain barrier, and therefore, is trapped irreversibly in brain according to the distribution of AChE enzyme activity.<sup>7–10</sup> Kinetic analysis of this radioactivity trapping provides a quantitative estimate of the regional AChE activity.<sup>11</sup> Statistically significant localized decreases have been observed in the cortical hydrolysis rate of [ $^{11}\text{C}$ ]AMP or [ $^{11}\text{C}$ ]PMP in moderate AD versus age-matched controls.<sup>2,3</sup> Also, [ $^{11}\text{C}$ ]PMP has been used to quantify AChE inhibition in rodents, primates, and humans.<sup>12–14</sup> These latter studies demonstrate the utility of PET radiotracers for AChE activity in evaluating the efficacy of new AChE inhibitors and optimizing the drug dosage schedule.

Based on these successes in using  $^{11}\text{C}$ -labeled PET radiotracers, a series of  $^{18}\text{F}$ -labeled PMP analogs has been studied.<sup>15,16</sup>  $^{18}\text{F}$ -labeled compounds would permit longer imaging times and allow the use of radiotracers with slower pharmacokinetics. This may provide improved measurement of enzymatic activity in brain regions with high AChE concentration. In those areas, the rapid rate of hydrolysis, combined with the high local concentration

**Keywords:** Fluorine-18; Acetylcholinesterase; Alzheimer's disease; PET.

\* Corresponding author. Tel.: +1 7349361183; fax: +1 7347640288; e-mail: [xshao@umich.edu](mailto:xshao@umich.edu)



**Table 2.** In vivo regional distribution in mouse brain

	PMP	1	2	3	4
Striatum	0.76 ± 0.13	0.35 ± 0.16	0.68 ± 0.29	0.38 ± 0.07	0.24 ± 0.15
Cortex	0.43 ± 0.08	0.34 ± 0.06	0.53 ± 0.15	0.34 ± 0.07	0.30 ± 0.16
Cerebellum	0.27 ± 0.08	0.26 ± 0.13	0.46 ± 0.11	0.35 ± 0.13	0.28 ± 0.19
Hippocampus	0.41 ± 0.09	0.37 ± 0.18	0.52 ± 0.15	0.36 ± 0.09	0.34 ± 0.20

Data are expressed as radioactivity retention fractions (mean ± SD,  $n = 4$ ) calculated as the ratio between radioactivity concentrations at 30 minutes and 1 minute post-injection of radiotracer.

to PMP. However, those retention fractions exhibited less distinction between cortex and cerebellum than observed for PMP. The ratio of cortex to cerebellum for compound **1** was 1.3, while the ratio for PMP was 1.6. The retention fractions of compound **2** were slightly higher than PMP in cortex, cerebellum, and hippocampus, consistent with the slightly more rapid cleavage of this radiotracer in brain. These data were still in agreement with the known distribution of AChE, striatum > cortex = hippocampus > cerebellum.<sup>13</sup> Again compound **2** exhibited less discrimination between regions than PMP. The striatum to cortex and cortex to cerebellum ratios for compound **2** were 1.3 and 1.2 compared to 1.8 and 1.6, respectively, for PMP. The retention fractions of compounds **3** and **4** were nearly uniform across all regions.

#### 2.4. Positron emission tomography imaging of rat brain

PET imaging studies were performed for PMP and <sup>18</sup>F-labeled radiotracers in male Sprague–Dawley rats ( $n = 3$  for each radiotracer) using a Concorde Microsystem (Knoxville, TN) R4 microPET scanner. The representative time–activity curves of the first 60 min for each radiotracer in striatum and cortex are shown in Figure

1. Data are normalized to the injected dose of radioactivity. All radiotracers, including PMP, showed a slow and constant washout from rodent brain not seen in primate. Compounds **1** and **4** showed significantly different kinetics in striatum as compared to PMP. Both tracers show high, rapid uptake followed by rapid and continuous clearance of radioactivity from striatum. Compound **1** exhibited similar clearance kinetics in cortex, whereas **4** was comparable to PMP in this region. Like the regional distribution in mouse brain, neither **1** nor **4** exhibited any differential retention of radioactivity in striatum versus cortex at later time points. The time–activity curve of compound **2** had similar kinetics to that of PMP in both striatum and cortex. Likewise the striatum versus cortex ratio for **2** at later time points was comparable to PMP. Compound **3** showed higher initial uptake than PMP in both regions but similar levels of clearance and kinetics. This large difference, as compared to PMP, between initial radioactivity uptake and retention of radioactivity at later time points is consistent with the lower retention fractions measured in mouse brain. These data also agree with the slower cleavage rate measured by purified enzymes and both in vitro and in vivo blood metabolism rates.

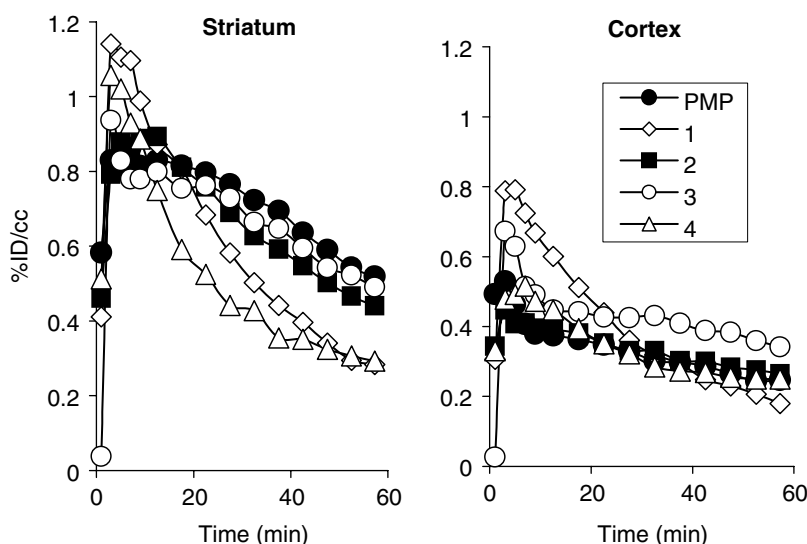


**Figure 1.** Rat striatum and cortex time–activity curve. Male Sprague–Dawley rats ( $n = 3$ ) were anesthetized using an isoflurane anesthesia machine and placed in plastic restrainer tubes secured on a microPET scanner (Robent R4 microPET, Concorde Microsystem Inc., Knoxville, TN). The animals were then injected with 2–4 mCi of radiotracer and imaged for 90 min. Data were acquired in list-mode and then rebinned as a sequence of five 2-min and 16 5-min frames. Regions of interest were created on frame 5 (8–10 min) of the dynamic sequence and applied to all other frames generating time–activity curves. Data were normalized to the injected dose of radioactivity. The first 60 min of imaging data from a representative experiment for each compound are shown.

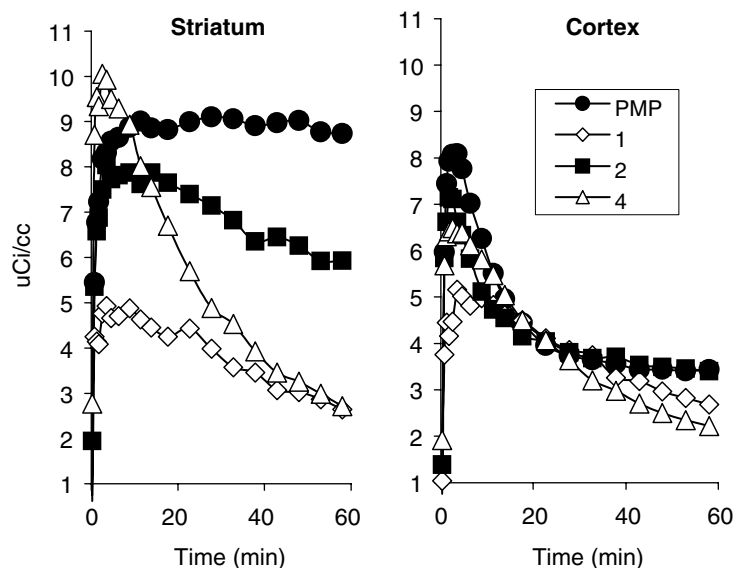


**Figure 2.** Primate striatum and cortex time-activity curve. Female pigtail monkey (*M. nemistrina*) was anesthetized (ketamine and xylazine) and secured on the gantry of a TCC PC 4600a tomography. The animal was then injected with 3–6 mCi of radiotracer and imaged for 90 min. Analysis of these image data was by method reported previously.<sup>11</sup> The first 60 min of data are shown.

## 2.5. Positron emission tomography imaging of primates

Using the reported protocol,<sup>7</sup> a female pigtail monkey (*M. nemistrina*) was injected with either **1**, **2**, or **4** and imaged for 60 min on a TCC PC4600a PET scanner. As reported by Zhang et al., the lower hydrolytic rate and lower specificity for AChE of this compound **3** may limit its usefulness for the quantitative measurement of AChE in the primate brain.<sup>16</sup> Therefore, the primate PET studies did not include this compound. Time-activity curves for striatum and cortex are shown in Figure 2, with previous PMP data included for comparison. Data are from a single PET study for each radiotracer but using the same animal for all scans. Data are normalized to the injected dose of radioactivity. In contrast to the rat imaging data, compound **1** showed a low initial uptake in primate brain. This likely reflects a more rapid cleavage of radiotracer in primate blood due to species differences in either cholinesterase concentration or selectivity. We have shown previously that more rapid metabolism of PMP analogs in blood results in less delivery of the radiotracer to brain.<sup>18</sup> No attempt was made in these initial primate studies to assess blood metabolism of radiotracers. As in the rodent studies, both **1** and **4** exhibited constant clearance of radioactivity from brain and no distinction between striatum and cortex. The cortex curve of compound **2** was nearly identical to that of PMP. The shape of the striatal curve for **2** showed some clearance of radioactivity from brain, indicating either slower hydrolysis kinetics, in contrast to the rodent studies, or incomplete trapping of radioactive metabolite.

The apparent hydrolysis rate constant  $k_3$  was calculated from these PET data using the no-input shape analysis reported previously, which does not require knowledge of the arterial input function.<sup>11</sup> This  $k_3$  value (shown in Table 3) reflects both the actual rate of enzymatic

**Table 3.** Hydrolysis rate constants  $k_3$

	PMP	1	2	4
Striatum ( $\text{min}^{-1}$ )	0.1009	0.0295	0.0487	0.0205
Cortex ( $\text{min}^{-1}$ )	0.0453	0.0299	0.0423	0.0234

The apparent hydrolysis rate constants  $k_3$  were calculated from PET data by reported method.<sup>11</sup>

hydrolysis and the local concentration of the enzyme. As with the retention fractions used in the mouse dissection studies, the shape analysis method depends on complete metabolism of radiotracer and trapping of the labeled metabolite. Thus  $k_3$  values calculated for **1** and **4**, both of which exhibit continuous clearance of radioactivity from brain, are unreliable. Compared to PMP, compound **2** showed a very similar  $k_3$  value in cortex, but a lower value in striatum. Additional studies will be required to determine the source of this discrepancy between rodent and primate data for **2**.

## 3. Discussion

*N*-[<sup>11</sup>C]Methyl-4-piperidiny] esters (AMP and PMP) have been characterized as synthetic acetylcholinesterase substrates for PET radiotracers, which upon hydrolysis form a <sup>11</sup>C-labeled metabolite that is essentially trapped within brain tissues.<sup>7</sup> Kinetic analysis of this rate of radioactivity trapping provides an estimate of AChE concentration in the given region.<sup>11</sup> As an ideal in vivo radiotracer for regional AChE activity in the brain, a <sup>18</sup>F-labeled analog of PMP is expected to enter into the brain freely,<sup>16</sup> be hydrolyzed specifically by AChE in vivo, and the tissue level of metabolite should reflect the relative proportion of enzyme activity present. Based on these requirements, a series of <sup>18</sup>F-labeled PMP analogs were designed and synthesized and the preliminary biological data were evaluated previously.<sup>15</sup> The results

were encouraging and these  $N$ -[ $^{18}\text{F}$ ]fluoroethyl compounds exhibited potential to be good PET radiotracers for measuring brain AChE activity. However, some discrepancies arose between in vitro and in vivo kinetics and there was an additional unknown metabolite observed in blood samples in vitro. In this study, we selected compounds **1–4** as radiotracer candidates and more in vivo experiments were performed.

As discussed previously, a proper hydrolysis rate is the key element for an AChE radiotracer such as PMP, since the current kinetic model depends on complete metabolism of the radiotracer in vivo. A rapid enzyme-mediated cleavage rate ( $k_3 \geq K_1$ ) causes delivery-dependence illustrated by the PMP striatum time-activity curve in Figure 2. The rapid uptake phase of this curve is followed by complete trapping of all radioactivity in brain tissue with little or no clearance of unmetabolized PMP. This delivery-dependent kinetics leads to excessive parameter variability. An excessively slow rate of metabolism ( $k_3 \ll K_1$ ) leads to a protracted clearance phase in which trapping of radioactive metabolite occurs over too long a time to be practical for short half-life radiotracers. As an estimate of cholinesterase-mediated cleavage, the in vivo blood and brain metabolism was examined for each compound. Compounds **1** and **4** exhibited very fast in vivo brain and blood metabolism likely due to the shorter distance from amine to carbonyl group in these molecules.<sup>17,18</sup> These compounds are hydrolyzed too rapidly to provide accurate measurement of brain AChE activity. Compounds **2** and **3** had both blood and brain in vivo metabolism rates comparable to those of PMP. The additional nonpolar radioactive metabolite observed with in vitro blood metabolism samples was not detected in blood or brain in vivo at late time points.<sup>15</sup> Such metabolites, if present, would have complicated the estimation of AChE activity in vivo. Compared to PMP, both compounds **1** and **2** had faster in vivo blood metabolism rates, while both compounds were hydrolyzed more slowly by purified enzyme than PMP and compound **2** showed a much slower in vitro blood metabolism rate than that of PMP.<sup>15</sup> The origin of this discrepancy is unclear. We have shown previously that the contribution of butyrylcholinesterase to the cleavage of these fluoroethyl derivatives is very small. One possibility is that clearance mechanisms contribute to in vivo blood metabolism that is faster than that of in vitro data. In this case, the clearance processes may prefer the fluoroethyl compounds, or its metabolite, to PMP. The exact mechanism of such a clearance preference is unclear. Also, the fluoroethyl compounds may be substrates for other nonselective carboxylesterases, which would result in a more rapid in vivo metabolism versus in vitro or assays with purified AChE. Therefore, additional enzyme selectivity assays will be required for full characterization of any radiotracer candidate to be used in human trials.

Calculation of regional retention fractions has been used as a simplified method for in vivo measurement of AChE activity in rodent brain.<sup>13</sup> This method, using [ $^{11}\text{C}$ ]PMP as a radiotracer, provided a measurement, with good sensitivity and reproducibility, for changes

of enzyme function. Compared to PMP, the retention fractions of all compounds exhibited less distinction between brain regions known to contain different AChE concentrations. That is, differences in radioactivity retention for **1**, **3**, and **4** did not represent the regional level of AChE activity as accurately as did PMP retention fractions. Only compound **2** exhibited retention fraction values in agreement with the known distribution of AChE in mouse brain: striatum > cortex = hippocampus > cerebellum,<sup>13</sup> but again with less distinction between brain regions than shown by PMP. However, the retention fraction method is based on the hypothesis that metabolism and irreversible trapping of hydrolyzed radiotracer is complete by 30 min. The microPET studies indicated that these fluoroethyl-compounds and their metabolites appear not to be completely trapped in the brain of rodents. These data indicate that, although the retention fraction method has provided a simple analysis of [ $^{11}\text{C}$ ]PMP pharmacokinetics, this method is not universally applicable to all AChE-substrate radiotracers.

Compounds **1** and **4** showed continuous clearance in microPET studies, likely due to the relatively higher lipophilicity of their labeled metabolites. The additional methylene group in compound **1** and its metabolite would add 0.519 log units to the octanol/water partition coefficient, based on fragmental constants for calculating log  $P$ .<sup>19</sup> This difference in lipophilicity may allow compound **1** and its metabolite to clear more rapidly from brain tissues, whereas the PMP metabolite is irreversibly trapped. Similarly the metabolite of **1** may partition back into brain from blood. The metabolite alcohol of compound **4** would also be expected to exhibit higher lipophilicity than either that of compound **3** or PMP based on the significantly different partition coefficients for  $N$ -methyl-3-piperidinol (log  $P$  = 0.015) and  $N$ -methyl-4-piperidinol (log  $P$  = 0.006).<sup>20</sup> This difference is likely caused by intramolecular hydrogen bonding.

Compound **3** had slower pharmacokinetics than others in vivo, which agreed with both in vitro hydrolysis rate and blood metabolism.<sup>15</sup> As reported by Zhang et al., the lower hydrolytic rate and lower specificity for AChE of this compound may limit its usefulness for the quantitative measurement of AChE in the primate brain.<sup>16</sup> Therefore, the primate PET studies did not include this compound.

Compound **2** showed time-activity curves in rat brain similar in shape to those of PMP in both striatum and cortex. This suggests again that **2** has potential to be a useful radiotracer for measuring brain AChE concentration. It should be noted that even the time-activity curve of PMP showed a slow constant clearance from rat brain. As previously reported, rat brain, unlike primate and human, does not irreversibly retain the enzyme-mediated cleavage product of PMP. Rather, this radio-labeled metabolite exhibited a slow clearance from all rat brain regions and thus likely could also enter the brain from blood.<sup>21</sup> This provided additional evidence that retention fractions in mouse brain might be



misleading. Thus, the primate studies were performed to determine whether this is truly a species difference or if clearance results from the *N*-fluoroethyl group's affect on lipophilicity. As shown in Figure 2, compounds **1** and **4** exhibit slow continuous clearance of radioactivity from primate brain. The time–activity curves for PMP and compound **2**, however, reach a plateau, albeit at 55 min for **2** in striatum. This argues that rodent blood–brain barrier is more permeable than that of primates and allows the radiolabeled metabolites of all of these radiotracers to clear from brain tissues. However, lipophilicity is also a factor in that the two less polar metabolites, of **1** and **4**, clear from both rodent and primate brain tissues.

The same protocol and kinetic analysis method reported for [ $^{11}\text{C}$ ]PMP primate studies was used to evaluate all fluoroethyl compounds.<sup>11</sup> The apparent hydrolysis rate constant  $k_3$  calculated from PET data reflects both the actual rate of enzymatic hydrolysis and the local concentration of the enzyme. Compound **1** showed a lower initial uptake in monkey brain. This is likely caused by rapid plasma metabolism and washout tendency. Compound **4** showed a different kinetic profile, with constant washout from both striatum and cortex. Both compounds **1** and **4** had lower primate  $k_3$  values than those of PMP. The obvious contribution of metabolite clearance kinetics ( $k_4$ ) indicates that the model formulation developed for PMP was not applicable for these compounds. Again this method is based on complete irreversible trapping of hydrolyzed radiotracer. Overall, these two radiotracers with their relatively fast in vivo hydrolysis rates and high lipophilicity may not be good candidate AChE substrates for use with PET.

Compound **2** showed a similar cortex time–activity curve to PMP. The striatal time–activity curve for **2** exhibited some clearance of radioactivity at early time points, but appears to approach a plateau after 55 min. The slower kinetics of **2** may be better for measurement of AChE activity in striatum, where high AChE concentration led to difficulties with delivery-dependent uptake for PMP. As reported previously in human [ $^{11}\text{C}$ ]PMP studies, the variability in  $k_3$  from statistical uncertainty was low (<10%) in cortex and jumped to 30% or greater for striatum.<sup>11</sup> Shape analysis of this curve yields an apparent striatal enzymatic rate constant  $k_3$  for compound **2** that was very close to that of PMP in primate cortex. However, longer imaging times will be necessary to determine whether the radioactive metabolite of **2** is indeed irreversibly trapped in striatal tissue, which is a requirement of this method.

#### 4. Conclusion

A series of  $^{18}\text{F}$ -labeled PMP analogs was evaluated as AChE substrates. Compounds **1** and **4** had relatively faster metabolism rates, faster clearance than PMP and poor discrimination between brain regions with different AChE concentration. Compound **3** showed a

slower blood metabolism, a slower pharmacokinetics, but again poor discrimination between brain regions. Compound **2** had highly encouraging characteristics with an in vivo metabolism rate, brain uptake and pharmacokinetics similar to PMP, and in addition, the apparently slower kinetics in primate striatum might allow better estimate of local AChE activity. This compound has potential to be a good PET radiotracer for measuring brain AChE activity.

### 5. Experimental

#### 5.1. Radiosynthesis

The syntheses of unlabeled (*S*)-*N*-fluoroethyl-2-piperidinemethyl acetate, (*R*)-*N*-fluoroethyl-3-pyrrolidinyl acetate, and *N*-fluoroethyl-4-piperidinyl acetate, as well as their radiolabeling precursors, have been reported previously.<sup>15</sup> (*R*)-*N*-fluoroethyl-3-piperidinyl acetate and the corresponding precursor were prepared using the same reported method.

A general procedure for synthesis of  $^{18}\text{F}$ -labeled fluoroethylpiperidine or pyrrolidine esters has been reported previously.<sup>15</sup> [ $^{11}\text{C}$ ]PMP was prepared using reported method.<sup>22</sup>

#### 5.2. In vivo blood and brain metabolism

Female CD-1 mice (20–25 g, Charles River Laboratories, Wilmington, MA) were anesthetized with diethyl ether and 500–1000  $\mu\text{Ci}$  of radiotracer was injected through the lateral tail vein. Animals were allowed to awaken then were re-anesthetized and sacrificed after 1, 15, and 30 min post-injection of radiotracer ( $n = 2$  at each time point). Blood was harvested (200  $\mu\text{L}$ ) from each mouse and mixed with 500  $\mu\text{L}$  of absolute ethanol. The whole brain tissues were removed and immediately homogenized in 1 mL of absolute ethanol. The samples of blood and brain were centrifuged and the supernatant was analyzed by thin-layer chromatography (TLC, silica, methanol/ $\text{CH}_2\text{Cl}_2$  2.5:97.5, concentrated  $\text{NH}_4\text{OH}$  in a small vial) at each time point. Radioactivity on the TLC plates ( $n = 2$  for each tissue from each animal) was quantified using a Fuji BAS-1800 phosphorimaging system. Regions of interest corresponding to authentic radiotracer, metabolite, and chromatographic origin were drawn manually.  $R_f$  values were 0.8 and 0.5 for authentic radiotracer and metabolite, respectively. The percentage of authentic radiotracer was calculated as the optical density of the authentic tracer region divided by the total signal in all regions.

#### 5.3. In vivo regional distribution in mouse brain

Female CD-1 mice (20–25 g, Charles River Laboratories, Wilmington, MA) were anesthetized with diethyl ether and 100–200  $\mu\text{Ci}$  of radiotracer was injected through the lateral tail vein. Animals were allowed to awaken then were re-anesthetized and sacrificed after 1 or 30 min post-injection of radiotracer ( $n = 4$  at each

time point). The brain was rapidly removed and dissected into samples of each brain region. Tissue samples were weighed and radioactivity counted for  $^{18}\text{F}$  using an automatic  $\gamma$ -counter (Packard Instrument, Meriden, CT). The radioactivity in each brain region was calculated as the percent injected dose per gram of tissue. The retention fraction for each radiotracer in each brain region was calculated from 1 and 30 min data according to the published method (see legend of Table 2).<sup>13</sup>

#### 5.4. Positron emission tomography imaging of rat brain

Male Sprague–Dawley rats (150–200 g; Charles Rivers Laboratories, Wilmington, MA) were anesthetized using an isoflurane anesthesia machine and placed on a micro-PET scanner (Rodent R4 microPET, Concorde Microsystem Inc., Knoxville, TN). The animal was then injected with 1–4 mCi of radiotracer and imaged for 90 min ( $n = 3$  for each radiotracer). Data were acquired in list-mode and then rebinned as a sequence of five 2-min and 16 5-min PET scans. Regions of interest were created on frame 5 (8–10 min) of the dynamic sequence and applied to all other frames generating time–activity curves. Data are normalized to the injected dose of radioactivity.

#### 5.5. Positron emission tomography imaging of primates

A female pigtail monkey (*M. nemistrina*) was anesthetized (ketamine and xylazine) and secured on the gantry of a TCC PC 4600a tomograph.<sup>7</sup> The animal was then injected with 3–6 mCi of radiotracer and imaged for 90 min. Analysis of these image data was performed using the same method as for the rat data.<sup>11</sup> A single animal study was performed for each radiotracer, but the same animal was used for all radiotracers. Data are normalized to the injected dose of radioactivity.

#### Acknowledgements

This work was supported by National Institutes of Health grant T-32-CA09015 (XS) and the Office of Science (BER), U.S. Department of Energy, Grant No. DE-FG02-87ER60561. We thank Phillip Sherman, George Kropog and James Moskwa for their assistance with the animal studies and the cyclotron staff at the University of Michigan PET Facility for radionuclide production.

#### References and notes

- Bierer, L.; Haroutunian, V.; Gabriel, S.; Knoott, P.; Carlin, L.; Purohit, D.; Perl, D.; Schmeidler, J.; Kanof, P.; Davis, K. *J. Neurochem.* **1995**, *64*, 749.
- Kuhl, D.; Koeppe, R.; Minoshima, S.; Snyder, S.; Ficaro, E.; Foster, N.; Frey, F.; Kilbourn, M. *Neurology* **1999**, *52*, 691.
- Shinotoh, H.; Namba, H.; Fukushima, K.; Nagatsuka, S.-L.; Tanaka, N.; Aotsuka, A.; Tanada, S.; Irie, T. *Alzheimer Dis. Assoc. Disord.* **2000**, *14*, S114.
- Volkow, N.; Ding, Y.; Fowler, J.; Gatly, S. *Biol. Psychiatry* **2001**, *49*, 211.
- Iyo, M.; Namba, H.; Fukushima, K.; Shinotoh, H.; Hagatsuka, S.; Suhara, T.; Sudo, Y.; Suzuki, K.; Irie, T. *Lancet* **1997**, *349*, 1805.
- Namba, H.; Iyo, M.; Fukushima, K.; Shinotoh, H.; Hagatsuka, S.; Suhara, T.; Sudo, Y.; Suzuki, K.; Irie, T. *Eur. J. Nucl. Med.* **1999**, *26*, 135.
- Kilbourn, M.; Snyder, S.; Sherman, P.; Kuhl, D. *Synapse* **1996**, *22*, 123.
- Irie, T.; Fukushima, K.; Akimoto, Y.; Tamagami, H.; Nozaki, T. *Nucl. Med. Biol.* **1994**, *21*, 801.
- Kilbourn, M.; Nguyen, T.; Snyder, S.; Sherman, P. *Nucl. Med. Biol.* **1998**, *25*, 755.
- Koeppe, R.; Frey, K.; Snyder, S.; Kilbourn, M.; Kuhl, D. *J. Cereb. Blood Flow Metab.* **1997**, *17*, S329.
- Koeppe, R.; Frey, K.; Snyder, S.; Phillipp, M.; Kilbourn, M.; Kuhl, D. *J. Cereb. Blood Flow Metab.* **1999**, *19*, 1150.
- Frey, K.; Koeppe, R.; Kilbourn, M.; Snyder, S.; Kuhl, D. *J. Nucl. Med.* **1997**, *38*, 146P.
- Kilbourn, M.; Sherman, P.; Snyder, S. *Nucl. Med. Biol.* **1999**, *26*, 543.
- Kuhl, D.; Minoshima, S.; Frey, F.; Foster, N.; Kilbourn, M.; Koeppe, R. *Ann. Neurol.* **2000**, *48*, 395.
- Shao, X.; Butch, E.; Kilbourn, M.; Snyder, S. *Nucl. Med. Biol.* **2003**, *30*, 491.
- Zhang, M.-R.; Furutsuka, K.; Maeda, J.; Kikuchi, T.; Kida, T.; Okauchi, T.; Irie, T.; Suzuki, K. *Nucl. Med. Biol.* **2002**, *29*, 463.
- Shao, X.; Lisi, J.; Butch, E.; Kilbourn, M.; Snyder, S. *Nucl. Med. Biol.* **2003**, *30*, 293.
- Snyder, S.; Gunupudi, N.; Sherman, P.; Butch, E.; Skaddan, M.; Kilbourn, M.; Koeppe, R.; Kuhl, D. *J. Cereb. Blood Flow Metab.* **2001**, *21*, 132.
- Mannhold, R.; Rekker, R. *Perspect. Drug Discovery Des.* **2000**, *18*, 1.
- Kikuchi, T.; Fukushima, K.; Ikota, N.; Ueda, T.; Nagatsuka, S.; Arano, Y.; Irie, T. *J. Labelled Compd. Radiopharm.* **2001**, *44*, 31.
- Irie, T.; Fukushima, K.; Ikota, N.; Namba, H.; Iyo, M.; Nagatsuka, S. *J. Labelled Compd. Radiopharm.* **1997**, *37*, 214.
- Snyder, S.; Tluczek, L.; Jewett, D.; Nguyen, T.; Kilbourn, M.; Kuhl, D. *Nucl. Med. Biol.* **1998**, *25*, 751.